Transactions of the Korean Nuclear Society Autumn Meeting
Gyeongju, Korea, October 29-30, 2015

Natural Convection Heat Transfer of Oxide Pool During In-Vessel Retention of Core Melts

Hae-Kyun Park and Bum-Jin Chung*
Department of Nuclear Engineering, Kyung Hee University
#1732 Deokyoung-daero, Giheung-gu, Yongin-si, Gyeonggi-do, 446-701, Korea
Corresponding author:bjchung@khu.ac.kr

1. Introduction

The reactor fuels are relocated at the lower plenum when a severe accident occurs. Then, the metal components and oxide fuels are separated by the density difference as metal layer and oxide pool, respectively. At this point, the integrity of reactor vessel may be threatened by the heat generation at the oxide pool and to the natural convection heat transfer to the reactor vessel by those two layers. Therefore, External Reactor Vessel Cooling (ERVC) is performed in order to secure the integrity of the reactor vessel. Whether the IVR(In-Vessel Retention) Strategy can be applicable to a larger reactor is the technical concern, which nourished the research interest for the natural convection heat transfer of metal and oxide pool and ERVC performance.

Especially, it is hard to simulate oxide pool by experimentally due to the high level of buoyancy. Moreover, the volumetrically exothermic working fluid should be adopted to simulate the behavior of the core melts. Therefore, the volumetric heat sources that immersed in the working fluid have been adopted to simulate oxide pool by experiment. We investigated oxide pool with two different designs of the volumetric heat sources that adopted previous experiments. The investigation was performed by mass transfer experiment using analogy between heat and mass transfers. The results were compared to previous studies.

2. Theoretical background

The volumetric heat sources have been introduced to simulate oxide pool by experiment in previous studies. Thus, the Ra'_H substituted to Ra_H to apply volumetric heating phenomenon as below:

$$Ra'_H = Ra_H \times Da \ , \tag{1}$$

$$\text{Damköhler number } (Da) = \frac{q'''H^2}{k\Delta T} \text{ and} \tag{2}$$

$$Ra'_H = \frac{g\beta\Delta TH^3}{\alpha\nu} \times \frac{q'''H^2}{k\Delta T} = \frac{g\beta q'''H^5}{\alpha\nu k}. \tag{3}$$

The different Ra'_H ranges and local heat transfer coefficient at the lower plenum were showed in the earlier studies.

Bonnet and Seiler [1] investigated the natural convection heat transfer of the oxide pool by experiment. They used 2D semicircular pool (BALI) as oxide pool and lattice shaped volumetric heat source with Ra'_H of 10^{15} – 10^{17}. The heat flux increased gradually along the curvature from the bottom and they developed heat transfer correlations for Nu of the top (Nu_{up}) and the curvature (Nu_{dn}) as below:

$$Nu_{up} = 0.383\ Ra'_H{}^{0.233} \text{ and} \tag{4}$$

$$Nu_{dn} = 0.116\ Ra'_H{}^{0.25}. \tag{5}$$

Sehgal *et al.* [2] investigated the natural convection heat transfer of the oxide pool using 2D semicircular pool (SIMECO). Two horizontal wires were adopted as volumetric heat source to achieve Ra'_H's of 1.51×10^{13} to 3.14×10^{13}. The heat transfer increased as the pool angle increased op to about 80 degrees from the bottom. Then, the heat transfer dropped at the angle of 90 degrees.

Lee *et al.* [3] investigated the natural convection heat transfer of oxide pool using two-dimensional semicircular pool (SIGMA CP). The bent wire electrode as S shape was used for volumetric heat source. The range of Ra'_H's were 5.71×10^6 to 7.04×10^{11}. The Nu's at the curvature increased as the angle of the pool increased. Meanwhile, the Nu's at the upper plate were varied with respect to positions. They also developed heat transfer correlations as below:

$$Nu_{up} = 0.31(Ra'_H Pr^{-0.36})^{0.245} \text{ and} \tag{6}$$

$$Nu_{dn} = 0.219(Ra'_H Pr^{-0.215})^{0.235}. \tag{7}$$

Suh *et al.* [4] used three-dimensional hemispherical pool (SIGMA 3D) to investigate the natural convection heat transfer of the oxide pool. The SIGMA 3D facility employed same design of the volumetric heat source as SIGMA CP. Range of Ra'_H from 4.46×10^6 to 3.5×10^{10} was established for experiments. The Nu's at the upper plate showed similar trends with SIGMA CP experiment. However, the Nu's at the curvature increased and dropped at the angle of 90 degrees as in the case of Sehgal *et al.* [2] which was not showed in the case of SIGMA CP experiment [3].

Palagin and Kretzschmar [5] investigated the natural convection heat transfer of oxide pool using 3D hemispherical pool (LIVE). The wires of ring array were employed as volumetric heat source and the Ra'_H was 1.2×10^{14}. The heat transfer at the curvature increased as the pool angle increased. However, the heat transfer of curvature over 77 degrees were not measured due to the low level of working fluid in the pool.

3. Experiments

3.1 Test matrix

Table 1. Test matrix for experiments.

Volumetric heat source	Pool top	Ra'_H
S-bend (SIGMA 3D)	Isothermal	3×10^{14}
	Adiabatic	
Ring (LIVE)	Isothermal	
	Adiabatic	

Table 1 is the test matrix of this experiment. Ra'_H is fixed value in order to compare two different volumetric heat sources. Two different shape of volumetric heat sources were adopted previous heat transfer studies [4-5]. The isothermal and adiabatic boundary conditions were established alternately. The lower plenum was kept isothermally in the all cases.

3.2 Methodology

The analogy between heat and mass transfers was applied for experimental methodology. Agar [6] figured out that correlations of mass transfer are similar to those of heat transfer under the same conditions. Since, the mathematical modeling of those transfer systems is same [7], the mass transfer results are able to substitute the heat transfer results. The analogy of dimensionless number is established also. *Nu* and *Pr* of heat transfer have analogy with *Sh* and *Sc* of mass transfer, respectively as listed in Table 2.

The electroplating system was attempted firstly by Levich [8] for the purpose of performing the mass transfer experiment. Moreover, Selman *et al.* [9] developed theory of applying electroplating system under different conditions. The study applied cupric acid copper sulfate (H_2SO_4–$CuSO_4$) electroplating system and limiting current technique for experimental performance was used. The current between electrodes is increases as the potential is increases, until the plateau region reaches where the current is stagnant in spite of the potential increase. The plateau section is termed as the limiting current. The cupper ion concentration on the cathode surface is regarded nearly zero. Therefore, mass transfer coefficient (h_m) could be calculated as below:

$$h_m = \frac{(1-t_{Cu^{2+}})I_{\lim}}{nFC_b} \quad (8)$$

Table 2. Dimensionless numbers for the analogous systems.

Heat transfer		Mass transfer	
Nu	$\frac{h_h H}{k}$	*Sh*	$\frac{h_m H}{D_m}$
Pr	$\frac{\nu}{\alpha}$	*Sc*	$\frac{\nu}{D_m}$
Ra	$\frac{g\beta\Delta T H^3}{\alpha\nu}$	*Ra*	$\frac{gH^3}{D_m\nu}\frac{\Delta\rho}{\rho}$

The isothermally cooled boundary conditions have to establish in order to investigate oxide pool by experiment. However, the cathode in terms of the mass transfer experiment has analogy with isothermally heated wall in terms of the heat transfer. Moreover, the limiting current technique is not able to apply for the anode [10]. Thus, the experimental facility of the mass transfer was overturned against the gravity direction for the purpose of establishing isothermally cooled wall by using limiting current technique. At this point, the originality of this research is that the isothermally cooled condition was established primally by mass transfer experiment.

3.3 Experimental facility

(a) S-bend heat source

(b) Ring heat source

(c) Lower head

(d) Top plate

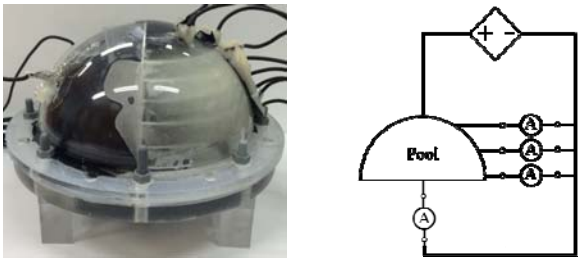

(e)Test rig (f) Experimental circuit

Fig. 1. Experimental facility.

Figure 1 shows experimental facility. The test rig composed of lower head and top plate. The segments of copper electrodes are placed on the inner surface of the lower head and the top plate. In order to gain local current values, the electrodes are composed of segments each half.

The lower head was filled with solution and capped by the top plate, which is combined with the anode as volumetric heat source. The multi-meters were connected with cathodes in parallel.

4. Results and discussion

4.1 Validation of piecewise value

Table 3. Current error of piecewise electrodes.

	Top cooled		Top insulated	
	S-bend	Ring	S-bend	Ring
Hemisphere	-3.2%	1.51%	-1.21%	-7.05%
Top	7.72%	10.25%	-	-

Table 3 shows the current measurement error between half-bulk and segments of electrodes. The maximum error was about 10%. In this respect, the measurement in segment electrodes had validation.

4.2 Comparisons with previous studies

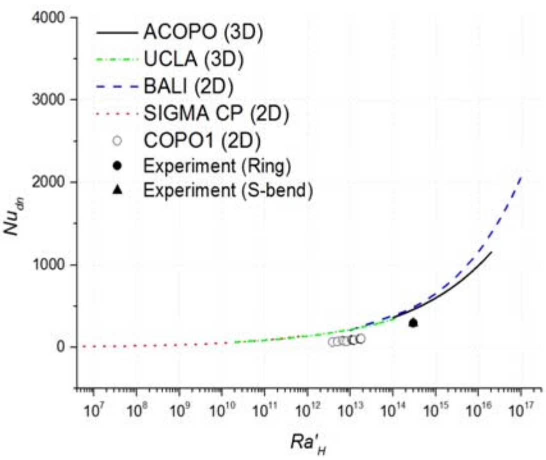

(a) Average downward *Nu*.

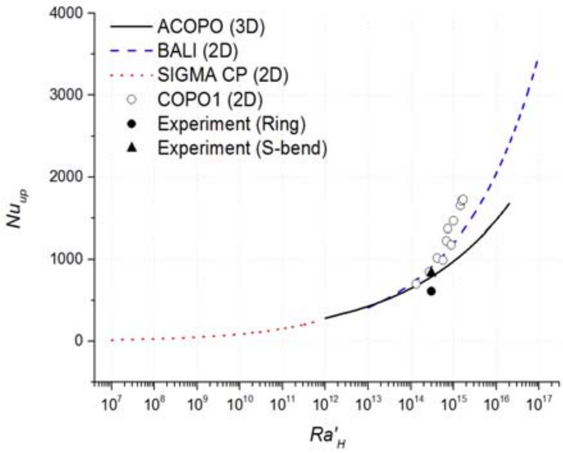

(b) Average upward *Nu*.

Fig. 2 Comparisons of *Nu* with respect to Ra'_H.

Figure 2 shows average *Nu*'s of this study and proceding. The all wall boundary conditions were isothermal cooling state. The Nu_{dn} of mass transfer result was in concordance with the proceding without slightly lower than that. The Nu_{up} of S-bend heat source was higher than that of ring heat source and was closer to proceding's. However, the S-bend heat source was located in the vicinity of the top plate, while ring heat source was not. The more delicate analyses for that reason will be realized in following part with respect to results of local Nu_{up}'s.

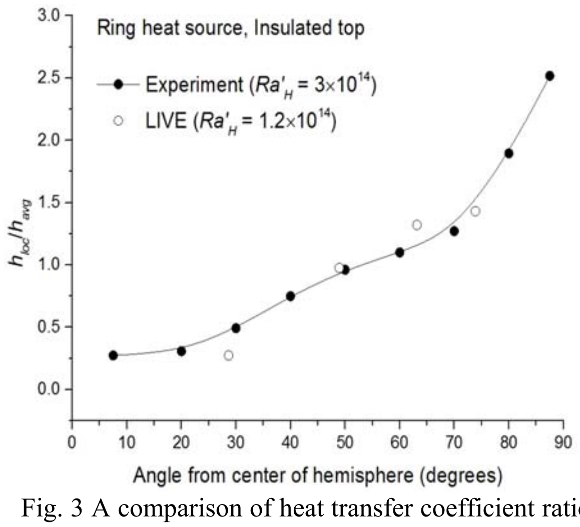

Fig. 3 A comparison of heat transfer coefficient ratio between mass transfer and LIVE experiment with respect to curvature angle.

Figure 3 is a comparison of heat transfer coefficient ratio of the lower plenum between this study and LIVE experiment [5]. The configurations of volumetric heat sources were identical and Ra'_H was order of 10^{14} both. The top plates kept in insulate condition. The heat transfer ratios of two results increased as curvature angle was increased. The slope of ratio decreased slightly in the vicinity of 60 degrees and increased steeply nearby 80 degrees in the case of mass transfer result. The thin boundary layer at high position was the main factor for the increase. Without high position results of LIVE experiment that was not measured, the two experiment results had similar heat transfer coefficient ratios.

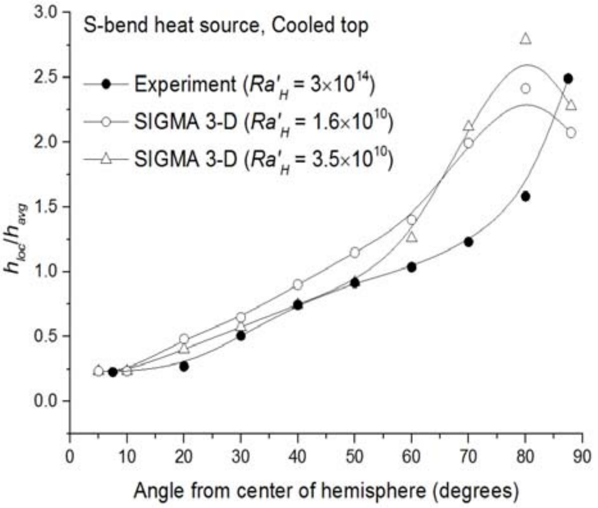

Fig. 4 A comparison of heat transfer coefficient ratio between mass transfer and SIGMA 3D experiment with respect to curvature angle.

Figure 4 is a comparison of heat transfer coefficient ratio of the lower plenum between this study and SIGMA 3D experiment [4]. The configurations of volumetric heat sources were identical and the all inner wall kept isothermal condition. The Ra'_H of experiment was over 10,000 times higher than SIGMA 3D experiment. The heat transfer coefficient ratios of two results increased as curvature angle was increased. The slopes of two results were similar under 60 degrees. However, the result of SIGME 3D was higher at 60 to 80 degrees and decreased steeply in the vicinity of the top plate. Sudden decrease of heat transfer at around 90 degrees is not expected as other phenomena are not involved. Thus this seems to be caused by the heat leakage of the SIGMA 3-D experiments at around 90 degrees. Therefore, the top plate of the SIGMA 3D experiment, which had thicker thermal boundary layer affects heat transfer of high position at the lower plenum.

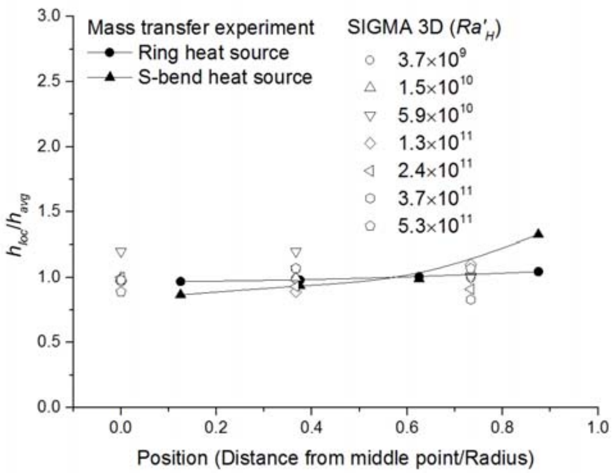

Fig. 5 A comparison of heat transfer coefficient ratio between mass transfer and SIGMA 3D experiment with respect to top position.

Figure 5 is a comparison of heat transfer coefficient ratio of the top plate between this study and SIGMA 3D experiment [4]. The ratio of S-bend heat source experiment increased as the far from the center with the range of 0.87 to 1.32. The scattered heat transfer coefficient ratios showed at the SIGMA 3D experiment. The variation ranges of the heat transfer coefficient ratios were similar between two S-bend and SIGMA 3D experiments. However, the ratio in the case of the ring heat source showed consistency regardless of the position. In this respect, the distance from volumetric heat source to the top plate affects the heat transfer of the top plate. The S-bend shaped heat source, which located much close to the top plate affects the convective flow in the vicinity of the top plate. Thus, flow disturbance caused the inconsistency result of S-bend and SIGMA 3D experiment.

5. Conclusion

We simulated the natural convection heat transfer of the oxide pool by mass transfer experiment. The isothermally cooled condition was established by limiting current technique firstly. The results were compared to previous studies under identical design of the volumetric heat sources. The average *Nu*'s of the curvature and the top plate were close to the previous studies. The local *Nu* at the curvature increased as the angle of the curvature increased. The range of Ra'_H will be varied in the further study and these 3D test rig results will compare to the results of 2D test rig in prospect.

ACKNOWLEDGMENT

This study was sponsored by the Ministry of Science, ICT and Future Planning (MSIP) and was supported by Nuclear Research and Development program grant funded by the National Research Foundation (NRF)

(Grant Code: 2014M2A8A1030777).

REFERENCES

[1] J. M. Bonnet and J.M. Seiler, Thermal hydraulic phenomena in corium pools: The BALI experiment, 7th International Conference on Nuclear Engineering, Tokyo, Japan, 1999.
[2] B. R. Sehgal *et al.*, SIMECO Experiments on In-Vessel Melt Pool Formation and Heat Transfer with and without a Metallic Layer, Division of Nuclear Power Safety, Royal Institute of Technology, Brinellvagen 60, 10044 Stockholm, Sweden.
[3] J. K. Lee et al., Experimental study of natural convection heat transfer in a volumetrically heated semicircular pool, Annals of Nuclear Energy, Vol.73, pp. 432-440, 2014.
[4] K. Y. Suh et al., In-vessel retention strategy for high power reactors, Korea Electrical Engineering & Science Research Institute, Korea, 2005.
[5] A. Palagin and F. Kretzschmar, LIVE test FSt4: experimental results and simulation by CONV code, The 13th International Topical Meeting on Nuclear Reactor Thermal Hydraulics, Knanazawa City, Japan, 2009.
[6] N. Agar, Diffusion and convection at electrodes, Discussion of Faraday Society, Vol.26, pp. 27-37, 1947.
[7] A. Bejan, Convection Heat Transfer, 3rd ed., John Wiley ＆ Sons, INC, New York, 2003.
[8] V. G. Levich, Physicochemical Hydrodynamics, Prentice Hall, Englewood Cliffs & NJ, 1962.
[9] J. R. Selman, *et al.*, Advances in Chemical Engineering, 10th, Academic Press, New York and London, 1978.
[10] Y. Konishi *et al*., Anodic dissolusion phenomena accompanying supersaturation of copper sulfate along a vertical plane copper anode, Electrochimica Acta, Vol.48, pp, 2615-2624, 2003.